

## Sol–gel template synthesis of $\text{LiV}_3\text{O}_8$ nanowires

Xiaohong Liu · Jinqing Wang · Junyan Zhang ·  
Shengrong Yang

Received: 22 December 2005 / Accepted: 20 March 2006 / Published online: 10 January 2007  
© Springer Science+Business Media, LLC 2007

**Abstract** The  $\text{LiV}_3\text{O}_8$  nanowires are fabricated by using sol–gel process with porous anodic aluminum oxide (AAO) as the template. Transmission electron microscopy (TEM) and scanning electron microscopy (SEM) characterizations show that the synthesized  $\text{LiV}_3\text{O}_8$  nanowires are monodispersed and paralleled to one another. Selected area electron diffraction (SAED) pattern, X-ray diffraction (XRD), and X-ray photoelectron spectroscopy (XPS) investigations jointly demonstrate that the synthesized nanowires are most consisted of monoclinic phase  $\text{LiV}_3\text{O}_8$ . Since the  $\text{LiV}_3\text{O}_8$  nanowires can be mass-produced by using this method, it is expected to find promising application as a new cathode material in lithium ion battery.

### Introduction

The discovery of carbon nanotube in 1991 [1] stimulated the research on one-dimension nanostructure materials, due to their special electronic, magnetic,

optical, and mechanical properties in comparison to their bulk counterparts [2–5]. Various methods have been developed to fabricate one-dimension nanostructure materials such as arc discharge, laser ablation, catalytic CVD growth, and template synthesis, etc [6]. Of those, template method is a convenient and inexpensive technique [7–12], especially, anodic aluminum oxide (AAO) templates possess very regular and highly anisotropic porous structures which offers a promising route to synthesize high surface area and ordered nanostructure materials. The ways used to synthesize the nano-materials in the pores of the template membranes include electroless metal deposition, electrochemical process, in situ polymerization, and sol–gel method [13–16]. Specially, the sol–gel process is a relatively easy and economical way to make uniform size and high quality stoichiometric targeted products. It has been demonstrated that sol–gel synthesis can be processed in the pores of the nanoporous template membranes to obtain nanowires, tubules, and fibrils of a variety of inorganic materials [16].

One-dimension nanostructure materials for using in the lithium ion battery have been extensively studied, in which cathode materials attract much attention [17–19]. As a candidate of cathode materials,  $\text{LiV}_3\text{O}_8$  was particularly focused on in the past 20 years due to its high capacity, facile preparation, and excellent stability in air. Various ways of preparing the  $\text{LiV}_3\text{O}_8$  material have been developed to enhance the electrochemical behavior, since Nassau and Murphy [20] realized that its electrochemical properties, such as discharge capacity, rate capacity, and cycle performances, could be strongly influenced by the preparation method. Hydrothermal, sol-gel, lower temperature synthesis,

---

X. Liu · J. Wang · J. Zhang · S. Yang (✉)  
State Key Laboratory of Solid Lubrication, Lanzhou  
Institute of Chemical Physics, Chinese Academy of  
Sciences, Lanzhou 730000, China  
e-mail: sryang@isl.ac.cn

J. Zhang  
e-mail: junyanzh@yahoo.com

X. Liu  
Graduate School, Chinese Academy of Science,  
Beijing 100039, China

and microwave synthesis, etc. have been widely used to prepare the  $\text{LiV}_3\text{O}_8$  cathode materials [21–28], while few study was reported on sol-gel synthesis of one-dimension  $\text{LiV}_3\text{O}_8$  nanostructures by using AAO as the template. In this work, high-ordered  $\text{LiV}_3\text{O}_8$  nanowire arrays are synthesized by using sol-gel-AAO template method for the first time. The structure and composition of the synthesized  $\text{LiV}_3\text{O}_8$  nanowire materials are characterized as well, which are expected to be used potentially as a new cathode material in lithium ion battery.

## Experimental

The precursor sol of  $\text{LiV}_3\text{O}_8$  was first synthesized. In detail, stoichiometric amounts of lithium nitrate and ammonium vanadate (the molar ratio of  $\text{Li}:\text{V} = 1:3$ ) were added slowly to deionic water with continuous stirring, then the solution was heated to  $80^\circ\text{C}$  following dropwise added with saturated citric acid, which was employed as a chelating agent, until the color of mixture changed from buff to brown, and finally became to dark blue. After stirring continually at  $80^\circ\text{C}$  for 4 h, a transparent sol was obtained. The prepared sol was very stable at room temperature and no precipitate was observed even for a long time.

The cleaned alumina membrane (Whatman anodisc, diameter = 47 mm) with pores diameter of approximately 200 nm and porosity of about 43%, was dipped into the prepared sol, and then the AAO template and sol system were transferred to a vacuum drier. After a desired time, the membrane was taken out from the drier, and the excess sol on the membrane surface was wiped off with a laboratory tissue. Finally, the

membrane was placed in an oven to dry at  $80^\circ\text{C}$  in air for 3 h followed by heat-treatment at  $450^\circ\text{C}$  for 20 h in a Muffle furnace, which resulted in the formation of  $\text{LiV}_3\text{O}_8$  nanowires inside the pores of the AAO template.

The morphology, composition, and crystallography of the  $\text{LiV}_3\text{O}_8$  nanowires were characterized. Transmission electron microscopy (TEM) images were obtained on a JEM-1200EX microscope to analyze the morphology and agglomeration of the nanowires. For TEM sample preparation, the alumina membrane was removed via dissolving with 3 M NaOH, and then diluted with deionic water. Droplets of suspension containing  $\text{LiV}_3\text{O}_8$  nanowires were placed onto the copper grids for TEM observation. Scanning electron microscopy (SEM) images were recorded with JSM-5600LV microscope. For SEM sample preparation, the alumina membrane with  $\text{LiV}_3\text{O}_8$  nanowires inside the pores was attached on a Cu cylinder. Then, a few droplets of 3 M NaOH were dropped on the sample to dissolve the membrane partially, and the samples were sputter-coated with gold prior to observation. The phase structure of as-synthesized nanowires with alumina membrane was determined on a D/max-RB X-ray diffractometer (Rigaku Corp., Tokyo, Japan) with  $\text{Cu-K}\alpha$  radiation at a scanning step size of  $2\theta = 0.017$ . The data were acquired in the  $2\theta$  range of  $10\text{--}80^\circ$ . The chemical states of typical elements of the nanowires with template membrane were analyzed on a PHI-5702 multi-functional X-ray photoelectron spectroscope (Physical Electronics, USA) operating with  $\text{Al-K}\alpha$  irradiation ( $h\nu = 1486.6\text{ eV}$ ) at a pass energy of 29.35 eV. The binding energy of contaminated carbon ( $\text{C}1s$ : 284.8 eV) was used as the reference and the resolution is about  $\pm 0.3\text{ eV}$ .

**Fig. 1** (a) TEM image of double  $\text{LiV}_3\text{O}_8$  nanowires after removing AAO template; (b) The corresponding selected area electron diffraction pattern for  $\text{LiV}_3\text{O}_8$  nanowires

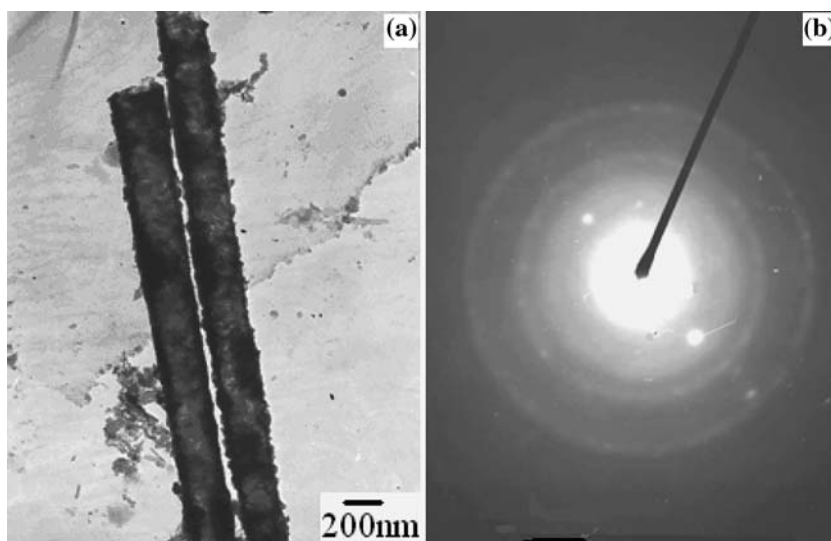
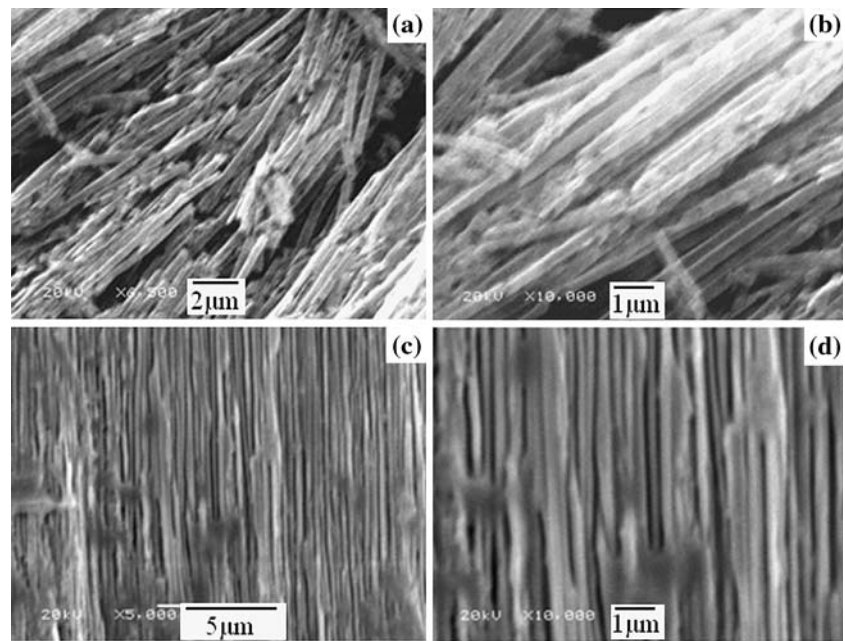


**Fig. 2** SEM images of  $\text{LiV}_3\text{O}_8$  nanowires arrays



## Results and discussion

The TEM images of the synthesized  $\text{LiV}_3\text{O}_8$  nanowires are shown in Fig. 1. It can be seen that two paralleled  $\text{LiV}_3\text{O}_8$  nanowires have a uniform diameter of 200 nm (Fig. 1a), which is in good agreement with the size of template pore. And, it is obvious that the nanowires are consisted of unnumbered nanoparticles, which is attributed to the fact that the growth mechanism of nanowires inside AAO template via sol–gel process is the nanoparticles deposition process in the pores of the AAO template [29]. Figure 1b gives the corresponding selected area electron diffraction (SAED) pattern taken from one above-mentioned nanowires. The diffraction rings, from inner to outer, correspond to the  $(-111)$ ,  $(112)$ ,  $(212)$ ,  $(312)$ , and  $(122)$  diffraction planes of  $\text{LiV}_3\text{O}_8$ , from which it can be concluded that the synthesized nanowires display polycrystalline structure and have well-defined monoclinic phase  $\text{LiV}_3\text{O}_8$ . This is identical with the results reported by Lin et al. [30, 31]. They have demonstrated that the nanotubes or nanowires prepared by the sol–gel method with AAO templates are polycrystalline.

The typical SEM images of  $\text{LiV}_3\text{O}_8$  nanowire arrays are shown in Fig. 2. Figure 2a is the image of  $\text{LiV}_3\text{O}_8$  nanowires isolated from AAO membrane. It can be seen that these nanowires are interlaced, piled, and possess uniform diameters, which indicates that this method could be used to mass-produce ordered  $\text{LiV}_3\text{O}_8$  nanowires. Figure 2b displays a cluster of  $\text{LiV}_3\text{O}_8$  nanowires arranged in the same direction for the residual AAO membrane, while Fig. 2c, d give the

cross-section surface images of the  $\text{LiV}_3\text{O}_8$  nanowire arrays at different magnification. It can be seen that the  $\text{LiV}_3\text{O}_8$  nanowire arrays are characterized by well distributed, high-ordered, and paralleled to one another, and few microscopic defects are found. This is attributed to that the alumina template membrane is only dissolved partially, which makes the nanowires like a brush anchored to the residual alumina membrane.

The X-ray diffraction (XRD) pattern of  $\text{LiV}_3\text{O}_8$  nanowire arrays within the alumina template membrane is shown in Fig. 3. Some diagnostic peaks are attributed to the monoclinic phase  $\text{LiV}_3\text{O}_8$  (JCPDS: 72-1193). They are assigned to  $(100)$ ,  $(-201)$ ,  $(200)$ ,

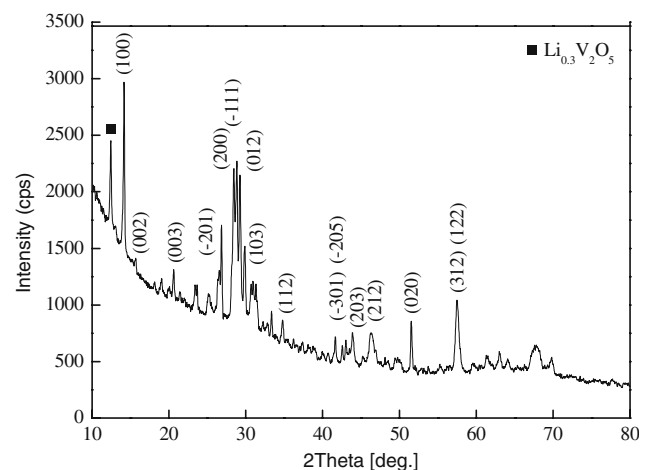


**Fig. 3** The XRD pattern of  $\text{LiV}_3\text{O}_8$  nanowires array with AAO template

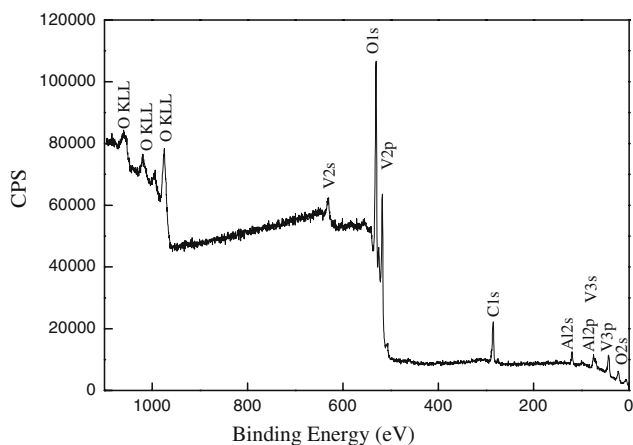


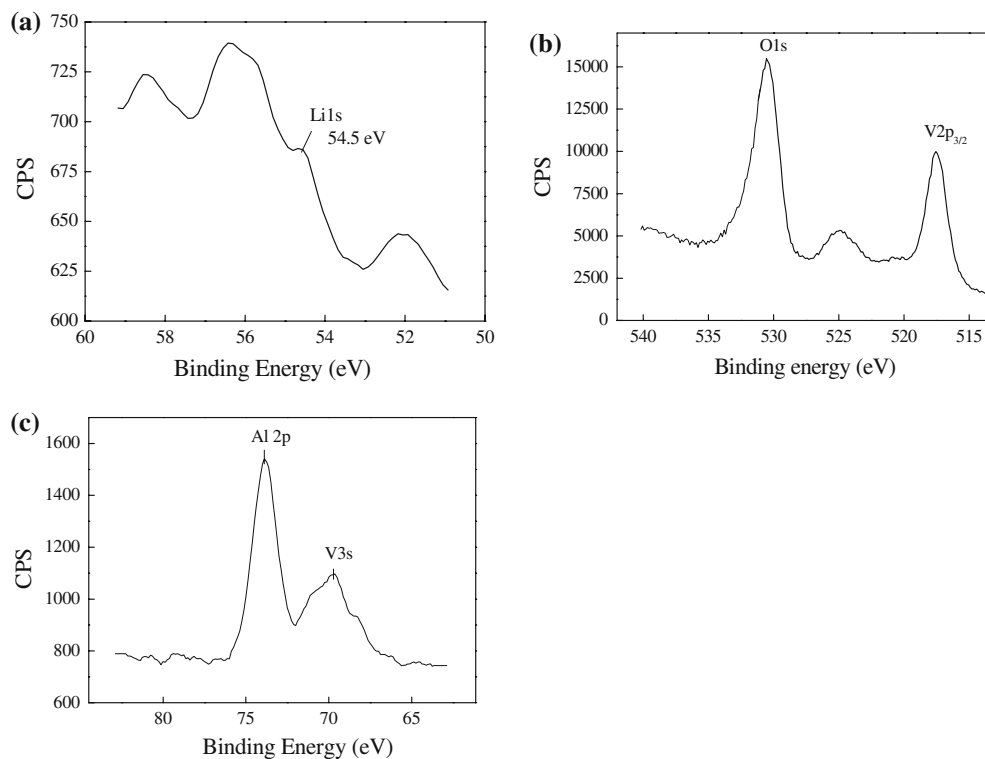
**Fig. 4** XPS survey spectrum of  $\text{LiV}_3\text{O}_8$  nanowires within the AAO template

( $-111$ ), ( $012$ ), ( $020$ ), ( $312$ ), and ( $122$ ) planes of  $\text{LiV}_3\text{O}_8$ , respectively, which are greatly consistent with the result of SAED analysis. Meanwhile, there is a diagnostic peak of  $\text{Li}_{0.3}\text{V}_2\text{O}_5$  appearing at  $2\theta = 12.4^\circ$ . But the intensity of peak is relatively weak comparing with that of the  $\text{LiV}_3\text{O}_8$ , indicating that the synthesized nanowire arrays are most consisted of monoclinic phase  $\text{LiV}_3\text{O}_8$ .

The chemical composition of the  $\text{LiV}_3\text{O}_8$  nanowires within the AAO template was also analyzed by XPS measurements. The survey scan XPS spectrum of the

prepared sample is shown in Fig. 4. It is clear that the signals of Li, V, and O are appeared on the spectrum. Figure 5 shows the high resolution XPS spectra of Li1s, V2p, Al2p, and O1s in the  $\text{LiV}_3\text{O}_8/\text{AAO}$  composite. The peak of Li1s at 54.5 eV (Fig. 5a) indicates that Li exists in the state of  $\text{Li}^+$ . It is well known that the binding energy of the  $\text{V}2\text{p}_{3/2}$  depends on the oxidation state of the vanadium cation, therefore XPS measurement can be used to detect the vanadium cation oxidation states. On the other hand, the binding energy of O1s is so close to that of  $\text{V}2\text{p}_{1/2}$  that the influence of O1s on V2p should be taken into account. Mendialdua et al. [32] reported that the oxidation degree of vanadium in vanadium oxide could be determined by using three parameters: the first is the energy difference ( $\Delta$ ) between the binding energy of O1s and  $\text{V}2\text{p}_{3/2}$ ; the second is the full width ( $\lambda$ ) at half maximum (FWHM); and the third is their peak shapes. In Fig. 5b, the  $\text{V}2\text{p}_{3/2}$  signal appears at 517.6 eV, and the energy difference is 12.9 eV, which are consistent with what have been reported by Silversmit et al. [33] where the  $\text{V}^{5+}$  binding energy is 517.7 eV, and the energy difference is 12.8 eV. Therefore, we can conclude reasonably that the V element in the synthesized  $\text{LiV}_3\text{O}_8$  nanowires is in a  $\text{V}^{5+}$  state. The O1s peak appeared at 530.5 eV comes from both  $\text{LiV}_3\text{O}_8$  and  $\text{Al}_2\text{O}_3$ . In Fig. 5c, we can see that the peak of Al2p appears at 73.9 eV corresponding to  $\text{Al}^{3+}$ , next to which is V3s peak appeared

**Fig. 5** XPS spectra of (a) Li1s; (b) O1s and V2p; and (c) Al2p core levels for the  $\text{LiV}_3\text{O}_8/\text{alumina}$  composite



at 69.2 eV. Considering all above XPS information along with the result of XRD, it is deduced that the synthesized nanowires is well-defined in the form of monoclinic  $\text{LiV}_3\text{O}_8$ .

## Conclusions

In summary, a simple process was developed to prepare well distributed and high-ordered  $\text{LiV}_3\text{O}_8$  nanowires by using sol-gel method with porous AAO as the template. TEM and SEM characterizations show that the synthesized nanowires are monodispersed and paralleled to one another, while XRD along with XPS investigations demonstrate that the synthesized nanowires are most consisted of monoclinic phase  $\text{LiV}_3\text{O}_8$ . This method offers the advantages of growing one-dimension  $\text{LiV}_3\text{O}_8$  nanowires in uniform size and unidirectional alignment, which are expected to be used as a potential cathode material in lithium ion battery.

**Acknowledgements** The authors would like to thank the National Natural Science Foundation of China (Grant No. 50375151, 50323007, and 50572107), 863 Plan (Grant No. 2002AA302609), and “Hundreds Talent Program” of Chinese Academy of Sciences for financial support.

## References

- Iijima S (1991) *Nature* 354:56
- Cui Y, Wei QQ, Park HK, Lieber CM (2001) *Science* 293:1289
- Huang Y, Duan X, Cui Y, Lauhon LJ, Kim KH, Lieber CM (2001) *Science* 294:1313
- Collins PG, Arnold MS, Avouris P (2001) *Science* 292:706
- Bachtold A, Hadley P, Nakanishi T, Dekker C, (2001) *Science* 294:1317
- Zhao WB, Zhu JJ, Chen HY (2003) *J Crystal Growth* 258:176
- Martin CR (1994) *Science* 266:1961
- Whitney TM, Jiang JS, Searson PC, Chien CL (1993) *Science* 261:1316
- Nguyen PP, Pearson DH, Tonucci RJ, Babcock K (1998) *J Electrochem Soc* 145:247
- Routkevitch D, Tager AA, Haruyama J, Almawlawi D, Moskovits M, Xu JM (1996) *IEEE Trans Electron Devices* 43:1646
- Hulteen JC, Martin CR (1997) *J Mater Chem* 7:1075
- Masuda H, Yanagishita T, Yasui K, Nishio K, Yagi I, Rao TN, Fujishima A (2001) *Adv Mater* 13:247
- Martin CR (1994) *Science* 166:1961
- Martin CR (1995) *Acc Chem Res* 28:61
- Martin CR (1996) *Chem Mater* 8:1739
- Lakshmi BB, Dorhout PK, Martin CR (1997) *Chem Mater* 9:857
- Zhou Y, Li H (2002) *J Solid State Chem* 165:247
- Zhou YK, Shen CM, Huang JE, Li HL (2002) *Mater Sci Eng B* 95:77
- Zhou YK, Shen CM, Li HL (2002) *Solid State Ionics* 146:81
- Nassau K, Murphy DW (1981) *J Non-Crystal Solid* 44:297
- Dai JX, Li SFY, Gao ZQ, Siow KS (1998) *J Electrochem Soc* 14:3057
- Scrosati B, Selvaggi A, Croce F, Gang W (1988) *J Power Sources* 24:287
- Yu A, Kumagai N, Lee JY (1998) *J Power Sources* 74:297
- Kawakita J, Kato T, Katayama Y, Miura T, Kishi T (1999) *J Power Sources* 81–82:448
- Pistoia G, Pasquali M, Wang G, Li L (1990) *J Electrochem Soc* 137:2365
- Liu GQ, Zeng CL, Yang K (2002) *Electrochim Acta* 47:3239
- Xu HY, Wang H, Sang ZQ, Wang YH, Yan H, Yoshimura M (2004) *Electrochim Acta* 49:349
- Yang G, Wang G, Hou WH (2005) *J Phys Chem B* 109:11186
- Li XX, Cheng FY, Guo B, Chen J (2005) *J Phy Chem B* 109:14017
- Lin Y, Sun FQ, Yuan XY, Geng BY, Zhang LD (2003) *Appl Phy A: Mater Sci Process* 78:1197
- Hernandez BA, Chang KS, Fisher ER, Dorhout PK (2002) *Chem Mater* 14:480
- Mendialdua J, Casanova R, Barbaux Y (1995) *J Electron Spectrosc* 71:249
- Silversmit G, Depla D, Poelman H, Marin GB, Gryse RD (2004) *J Electron Spectrosc* 135:167